



ORIGINAL ARTICLE

Development of glycyrrhetic acid ligand-functionalized liposomes for targeting hepatocellular carcinoma: Synthesis, preparation, characterization, and evaluation



Yuan Lin ^{a,1}, Yimin Zhang ^{a,c,1}, Zhuang Xiong ^a, Min Wu ^a, Muling Zeng ^a,
Chuangnan Li ^d, Fujin Liu ^a, Yazhi Liao ^a, Chunping Liu ^{e,f,g,*}, Jing Chen ^{a,b,*}

^a School of Biotechnology and Health Sciences, Wuyi University, Jiangmen 529020, China

^b International Healthcare Innovation Institute (Jiangmen), Jiangmen 529020, China

^c International Institute for Translational Chinese Medicine, Guangzhou University of Chinese Medicine, Guangzhou 510006, China

^d Neurosurgery Department, Jiangmen Wuyi Hospital of TCM, Affiliated Jiangmen TCM Hospital of Jinan University, Jiangmen 529020, China

^e State Key Laboratory of Dampness Syndrome of Chinese Medicine, The Second Affiliated Hospital of Guangzhou University of Chinese Medicine, Guangzhou 510080, China

^f Guangdong-Hong Kong-Macau Joint Lab on Chinese Medicine and Immune Disease Research, Guangzhou 7510080, China

^g State Key Laboratory of Quality Research in Chinese Medicine, Institute of Chinese Medical Sciences, University of Macau, 999078, Macau, China

Received 12 February 2023; accepted 1 July 2023

Available online 7 July 2023

KEYWORDS

Ligand synthesis;
GA-DA-CH;
Liposomal preparation;
Physicochemical characterization;
Hepatocellular-targeting

Abstract In this study, we successfully synthesized a novel glycyrrhetic acid (GA) derivate compound as a liposomal carrier. Glycyrrhetic acid-diaminododecane-cholesterol (GA-DA-CH) was synthesized from GA, diaminododecane, and cholesteryl hemisuccinate by two-step amidation under catalytic conditions. The chemical structures of GA-DA (glycyrrhetic acid-diaminododecane) and GA-DA-CH were confirmed by Mass Spectrum (MS), Nuclear Magnetic Resonance (NMR) spectrometer, and analyzed by Fourier Transform Infrared spectroscopy (FTIR), High-Performance Liquid Chromatography (HPLC). Glycyrrhetic acid ligand-modified liposomes (GA-DA-CH-Lips) were prepared, consisting of egg phosphatidylcholine,

* Corresponding authors.

E-mail addresses: chunpingliu@gzucm.edu.cn (C. Liu), wuyuchemcj@126.com (J. Chen).

¹ These authors contributed equally to this work.

Peer review under responsibility of King Saud University.



cholesterol and GA-DA-CH. GA-DA-CH was integrated into the liposomal capsule to promote hepatocellular carcinoma targeting. The particle size of GA-DA-CH-Lips was calculated to be between 122.87 and 133.30 nm, with an approximate polydispersity index (PDI) was 0.20, and a zeta potential was in the range of -32.50 to -26.53 mV. GA-DA-CH-Lips were constructed with more than 90% encapsulation efficient and drug loading efficiency of no $< 6.40\%$. In addition, environmental stability assays show that GA-DA-CH-Lips are sensitive to temperature, and thus should be preserved at low temperatures. Furthermore, *in vitro* cellular uptake from qualitative and quantitative analysis indicates that GA-DA-CH integrating into liposomes possess a specific target for hepatocellular carcinoma. Intracellular inhibition showed that GA-DA-CH-Lips effectively inhibited cell proliferation in dose-dependent features. Based on these results, we have reason to believe that GA-DA-CH-Lips could be a potential hepatic target drug delivery to improve the therapeutic effect of hepatic diseases.

© 2023 The Author(s). Published by Elsevier B.V. on behalf of King Saud University. This is an open access article under the CC BY license (<http://creativecommons.org/licenses/by/4.0/>).

1. Introduction

With an estimated 905,677 new cancer cases and 830,180 deaths, liver cancer is the sixth most commonly diagnosed cancer worldwide, and the third leading cause of cancer mortality in 2020 (Sung et al., 2021), seriously threatening human health and social development. Overall, liver cancer is a general denomination, and each form of cancer is named after the cell type that becomes cancerous. In particular, hepatocellular carcinoma is the most frequently occurring type of primary liver cancer, representing approximately 75–85% of all cases and resulting in more than 700,000 deaths per year worldwide (Paganoni et al., 2021; Sung et al., 2021). There are some conventional therapeutic options for hepatocellular carcinoma treatment, including tumor excision (Aoki et al., 2020; Cucchetti et al., 2020), radiotherapy (Kamimura et al., 2021), chemotherapy (Hou et al., 2022; Yamamoto et al., 2018), liver transplantation (Kim et al., 2020; Kakos et al., 2022), ablation therapy (Li et al., 2019; Yamagishi et al., 2019), and transarterial chemoembolization (Guo et al., 2022). However, the major issue associated with the administration of chemotherapeutic options is that they easily destroy normal tissues because of their poor specificity and systemic toxicity. Therefore, there is an urgent need to develop specific-targeting nanomaterials in drug delivery system for hepatocellular carcinoma treatment.

Licorice, one of the most popular herbal medicines in China, has widespread application in Chinese medicine (Pastorino et al., 2018). GA is a main bioactive compound extracted from the root and rhizome of licorice (Lekar et al., 2019; Tikhomirova et al., 2010). Modern pharmacological studies have proved that GA has therapeutic effects on various cancers such as liver cancer (especially hepatocellular carcinoma) (Chen et al., 2018), pancreatic cancer (Sun et al., 2020), gastric cancer (Cai et al., 2018), breast cancer (Sharma et al., 2012), and lung cancer (Luo et al., 2021). The GA binding site has strong affinity for a particular fraction of liver, which plays a significant role in liver through specific binding proteins named “GA receptors” (Negishi et al., 1991). GA is regarded as an important biofilm factor in hepatocyte membranes. Many reports have confirmed that there are highly specific GA and glycyrrhizic acid binding sites on the liver cell membrane (Negishi et al., 1991; Speciale et al., 2022; Stecanella et al., 2021). In particular, the number of GA binding sites was far more than that of glycyrrhizic acid binding, which indicated that GA receptors are more effective than glycyrrhizic acid receptors for targeting hepatocellular carcinoma (Cai et al., 2016; Negishi et al., 1991). As a result, GA is found in high abundance on the cellular membrane of hepatocytes (Cai et al., 2016; Wu et al., 2020). By combining this information, we provide a new insight into GA as a functionalized material to specifically target hepatocellular carcinoma sites, thereby reducing the accumulation of chemotherapeutic drugs in normal hepatocytes.

Nano-based drug delivery systems such as liposomes, nanoparticles, polymer micelles, and dendrimers were widely applied to encapsulate functional molecules for tumor targeted therapy, which exhibited outstanding properties, such as targeted delivery, and site-specific release (Mu et al., 2020; Seidi et al. 2018). Among the available nano-based drug delivery systems, liposomes are a promising strategy for cancer targeted therapy because of the approval of many liposomal formulations for clinical application (Beltrán-Gracia et al., 2019). These liposomes are bilayer vesicles composed of phospholipids and cholesterol, which possess the advantages of biocompatibility, biodegradability, non-toxic and non-immunogenicity (Guimaraes et al., 2021). However, the passive nature of liposomal drug delivery is vulnerable to phagocytosis by the reticuloendothelial system. Conventional liposomes have certain disadvantages, including the lack of tumor specificity and insufficient uptake at solid tumors. To overcome these shortcomings, we attempt to develop active targeting approaches involved the attachment of advanced functionalities such as targeting ligands on the surface of liposomes for enhanced delivery of liposomal systems. Previous studies have demonstrated that modifying liposomes with liver-targeting ligands containing GA compounds could improve drug concentration in hepatocellular cells (Huang et al., 2020; Zhao et al., 2021). Taking all this into account, GA has been used as a ligand due to the abundance of GA receptors expressed on the sinusoidal surface of mammalian hepatocellular carcinoma to enhance drug accumulation (Lv et al., 2017; Yan et al., 2018). GA-modified liposomes can therefore target hepatocellular carcinoma to enhance drug accumulation.

The aim of this study to prove that development of GA ligand modified liposomes as an advanced functional nanomaterial could actively target hepatocellular carcinoma. GA-DA-CH consisted of three parts: GA, diaminododecane, and cholesteryl hemisuccinate. GA was used as a binding molecule for GA receptors. Cholesteryl hemisuccinate containing cholesterol was one of the liposomal components to enhance the stability of liposomes. Diaminododecane was a linker between GA and cholesteryl hemisuccinate. A target molecule of GA-DA-CH was successfully synthesized, and then GA-DA-CH-modified liposomes (GA-DA-CH-Lips) were prepared by thin-film method. In addition, the physicochemical properties and stability of the functionalized liposomes were characterized. We then further aimed to confirm whether GA-DA-CH-Lips possessed target efficiency. Bioactivity evaluations *in vitro* were performed, via the hepatocellular inhibitory assay and cellular uptake efficiency of GA-DA-CH-Lips. The results favor our hypothesis that GA-DA-CH mediated liposomes can improve cellular uptake of drug by GA receptor-expressing HepG2 cells, indicating that GA-DA-CH is a promising GA ligand functionalized liposome.

2. Materials and methods

2.1. Materials, cells

GA (assay 99%), 1,12-diaminododecane (assay 99%), cholesteryl hemisuccinate (assay 97%), N,N-diisopropylethylamine (DIPEA, assay 99%), O-(7-azobenzotriazol-1-yl)-N,N,N',N'-tetramethylurea-hexafluorophosphate (HATU), 1,3-dicyclohexylcarbodiimide (DCC, assay 99%), N,N-dimethylformamide (DMF, assay 99%), anhydrous sodium sulfate (assay 99%), sodium chloride (assay 99.8%), dichloromethane (DCM, assay 99%), pyridine (assay 99.5%), coumarin-6 were all purchased from Aladdin Industrial Corporation (Shanghai, China). Egg phosphatidylcholine (assay 98%) and cholesterol (assay 98%) were purchased from Advanced Vehicle Technology Pharmaceutical, Co., Ltd. (Shanghai, China). 4',6'-diamidino-2-phenylindole (DAPI), paraformaldehyde, methyl thiazolyl tetrazolium (MTT) were purchased from Shanghai Biyuntian Biotechnology Co., Ltd. (Shanghai, China). Sephadex G-50 was obtained from Amersham Pharmacia Biotech (Piscataway, USA). Methanol (HPLC grade) was purchased from Oceanpak Alexative Chemical, Ltd (Goteborg, Sweden). All other reagents were of analytical grade.

HepG2 cells were cultured in Dulbecco's modified Eagle's medium (DMEM, GIBCO Life Technologies Corp, Carlsbad, USA) with 10% fetal bovine serum (FBS) at 37 °C in a humidified incubator containing with 5% CO₂. The cells were maintained in their exponential growth phase.

2.2. Synthesis of GA-DA-CH

The synthetic reaction of GA-DA-CH was performed via two steps. For the first step, GA-DA was synthesized. GA (4.25 mmol), was added into a round-bottom flask (100 mL), and then HATU (4.25 mmol), DMF (15 mL) and DIPEA (1.48 mL) were added under magnetic stirring for 30 min at 0 °C. Then 1,12-diaminododecane (4.67 mmol) was added. The reactions occurred at 26 °C without oxygen, and the reaction time was 4 h. The organic solvent was removed by the liquid-liquid extraction method (ethyl acetate : deionized water = 1:1, v/v). Anhydrous sodium sulfate was added to the collected organic medium to remove water. GA-DA was separated from the synthetic liquid by silica gel column chromatography. Ethyl acetate and petroleum ether (2:1, v/v) were chosen as eluant. In the second step, the synthesis of GA-DA-CH was synthesized in non-aqueous medium. Cholesteryl hemisuccinate (0.1027 mmol) and DCC (0.1844 mmol) were added into a round-bottom flask (50 mL), and then DCM (5 mL) was added under magnetic stirring at 26 °C. In addition, GA-DA (0.1537 mmol), DCM (5 mL) and pyridine (40 µL) were added into a reaction beaker and stirred for 5 min at 26 °C, and then the mixture was transferred into the above round-bottom flask. 5 mL DCM was added to the reaction and the synthesis process occurred without oxygen by nitrogen protection for 24 h. The crude product was obtained by the liquid-liquid extraction method. The organic phase was separated from the mixture solvents of DCM : hydrochloric acid (1:1, v/v), and then the organic phase was added into the aqueous phase (saturated sodium bicarbonate solution). Thin-layer chromatography (TLC) was used for

identification in a silica gel G plate with cyclohexane-ethyl acetate ether (3:1, v/v) as a developing solvent. GA-DA-CH was separated by silica gel G column chromatography with gradient elution including pure petroleum ether, cyclohexane-ethyl acetate (10:1, 8:1, and 5:1, v/v). The purified GA-DA and GA-DA-CH were analyzed by MS and NMR spectroscopy. The data is shown below:

Data of GA-DA:

ESI-MS (*m/z*): 653.5610 [$M + H$]⁺ calcd for C₄₂H₇₂N₂O₃ ([M] = 652.5543). ¹H NMR (500 MHz, CDCl₃, *ppm*) δ 5.74 (t, *J* 5.7 Hz, 1H), 5.64 (s, 1H), 4.11 (q, *J* 7.1 Hz, 1H), 3.24 (m, 2H), 2.77 (d, *J* 13.5 Hz, 1H), 2.32 (s, 1H), 1.93 (d, *J* 12.8, 2.9 Hz, 1H). ¹³C NMR (126 MHz, CDCl₃, *ppm*): δ 200.19, 175.58, 169.41, 128.45, 78.73, 61.82, 54.94, 48.17, 45.37, 43.56, 43.24, 41.80, 39.52, 39.15, 37.50, 37.07, 32.76, 31.91, 31.52, 29.76, 29.67, 29.41, 29.19, 28.53, 28.12, 27.28, 26.90, 26.47, 26.41, 23.37, 18.68, 17.49, 16.37.

Data of GA-DA-CH:

APCI-MS (*m/z*): 1119.7506 [$M - H$]⁻ calcd for C₇₃H₁₂₀N₂O₆ ([M] = 1120.9146). ¹H NMR (500 MHz, CDCl₃, *ppm*): δ 7.17 (s, 1H), 5.34 (m, 1H), 4.59 (m, 1H), 3.68 (m, 1H), 2.67 (m, 4H). ¹³C NMR (126 MHz, CDCl₃, *ppm*): δ 173.11, 173.02, 154.05, 130.03, 122.73, 74.63, 64.35, 56.71, 56.13, 50.04, 42.31, 39.72, 39.52, 38.06, 36.96, 36.60, 36.18, 35.79, 33.38, 32.51, 31.91, 31.84, 30.75, 30.70, 30.66, 29.87, 29.71, 29.68, 29.54, 29.33, 28.23, 27.70, 27.23, 27.18, 26.18, 25.50, 25.37, 24.68, 24.45, 24.28, 23.82, 22.83, 22.70, 22.57, 21.03, 19.30, 19.14, 18.72, 11.86.

2.3. FTIR analysis of GA-DA-CH

The FTIR of GA-DA-CH was obtained on a Nicolet 6700 FTIR spectrophotometer (Thermo Scientific Nicolet iS10, USA). GA-DA-CH (1–2 mg) and potassium bromide (mass ratio = 1:100) was mixed by an agate mortar and compressed into a thin-disk. Infrared spectroscopy in the range of 4000–400 cm⁻¹ in transmission mode was used to obtain characteristic peaks.

2.4. HPLC method for the analysis of GA-DA-CH

The content of GA-DA-CH was assessed by HPLC (Acquity Arc, Waters, USA) using a mixture of 5 % cyclohexane in methanol as mobile phase, with a flow rate of 1 mL/min in an XBridge®C18 Column, 250 × 4.6 mm, 5 µm column (Waters, USA). The injection volume was 10 µL and the detection signal was recorded at 210 nm (ultraviolet lamp) keeping the analysis system at room temperature.

2.5. Liposomes preparation

GA-DA-CH-Lips were prepared by the film dispersion method (Chen et al., 2021; Ye et al., 2019). Briefly, egg phosphatidylcholine and cholesterol (9:1, mass ratio) and GA-DA-CH (GA-DA-CH : phosphatidylcholine = 2:25, mass ratio) were dissolved in chloroform (5 mL). The solvent was then evaporated by a rotary evaporator (RE-2000, Shanghai Yarong Biochemistry Instrument Factory, Shanghai) to remove organic

solvent. A thin film was formed on the inner walls of the round-bottom flask. The lipid film was subsequently hydrated with phosphate-buffered saline (PBS, pH 7.4) for 30 min at 40 °C, and the liposomal suspensions were homogenized for 10 min at 10000 rpm in ice bath using a high speed dispersion homogenizer (FJ-200, Shanghai, China). Finally, liposomal suspensions of GA-DA-CH-Lips were passed through 0.22 µm polycarbonate filters and stored in a seal container at 4 °C.

Blank liposomes (B-Lips) were prepared in a similar way without GA-DA-CH. To investigate the cellular uptake of GA-DA-CH, coumarin-6 was chosen as a fluorescent probe to label the preparations. The fluorescent liposomes (Cou6-Lips and Cou6-GA-DA-CH-Lips) were prepared using the same procedures as described for the GA-DA-CH-Lips. The mass ratio of lipid and coumarin-6 was 100:1.

2.6. Physicochemical characterization of GA-DA-CH-Lips

2.6.1. Morphological measurement

The structure and morphology of GA-DA-CH-Lips were characterized by transmission electron microscopy (TEM), as described previously (Zhu et al., 2021). The prepared liposomal suspensions were diluted 10-fold with deionized water, a drop of diluted dispersion was placed on a copper grid, and then the excess sample was removed. The sample was negatively stained with phosphotungstic acid for 10 min at room temperature before further analysis. The particle morphology of GA-DA-CH-Lips was observed under the TEM.

2.6.2. Particle size, PDI, and zeta potential analysis

The particle size, PDI, and zeta potential of GA-DA-CH-Lips were measured by using previously reported methods (Zhu et al., 2018; Huang et al., 2020). These were determined using a modular dynamic light scattering particle analyzer (Microtrac Inc, Germany). The samples of GA-DA-CH-Lips were diluted with 5-fold distilled water before measurement to avoid the multiple scattering effects. Each sample was analyzed in triplicate at 25 °C.

2.6.3. Encapsulation efficiency and drug loading analysis

Encapsulation efficiency and drug loading of GA-DA-CH-Lips were measured using the Sephadex-50 filtration method (Chen et al., 2017). Liposomal suspension (1 mL) was filtered a Sephadex-50 mini-column (1.5 × 22 cm), and the distilled water fraction containing the liposomes of encapsulated GA-DA-CH (5 mL) was collected. The number of liposomes containing GA-DA-CH or encapsulated ligands was collected and analyzed by HPLC. Encapsulation efficiency was expressed as the ratio of liposome encapsulated GA-DA-CH to the total amount of ligands. Drug loading was expressed as the percentage of liposome encapsulated GA-DA-CH to the total amount of blank liposomes and ligands.

2.7. Stability of GA-DA-CH-Lips

The stability of GA-DA-CH-Lips was determined under different storage conditions, as reported previously (Huang et al., 2020; Chen et al., 2022). Liposomal samples stored at 26 °C and 4 °C for 28 days were used to study their stability

characteristics. At prescribed time intervals (0 d, 7 d, 14 d, 21 d, and 28 d), the characteristics of GA-DA-CH-Lips, including particle size, encapsulation, and drug loading were measured by using the above methods. Each sample was repeated in triplicate.

2.8. In vitro cellular uptake of GA-DA-CH-Lips

To evaluate the targeting efficiency of GA-DA-CH in HepG2 cells, coumarin-6 was used as a fluorescent indicator, and fluorescent liposomes (Cou6-GA-DA-CH-Lips, Cou6-Lips) were prepared. The cell uptake was analyzed qualitatively by a fluorescence microscope and quantitatively by a fluorescence microplate as described previously (Farooq et al., 2021; Chen et al., 2021). The cellular uptake of Cou6-GA-DA-CH-Lips modified different concentrations of coumarin-6 (0.1 µg/mL and 0.2 µg/mL) was studied. HepG2 cells were seeded in 24-well plates at a density of 5.0×10^4 cells per well with 10% FBS containing medium for at 37 °C for 24 h. The medium was removed and replaced with Cou6-GA-DA-CH-Lips, Cou6-Lips. After incubation for 4 h, the cells were washed with cold PBS solution and fixed with 4% paraformaldehyde solution for 20 min. These cells were dyed with 10 µL DAPI for 20 min, the dyestuff was discarded, and each well was washed with PBS. Fluorescence intensity of Cou6-GA-DA-CH-Lips was observed under a fluorescence microscope. The quantitative experiment was performed according to previously published protocols (Chen et al., 2017). HepG2 cells were divided into two groups of Cou6-Lips and Cou6-GA-DA-CH-Lips, which were cultured in an incubator for 4 h, following the addition of samples containing different concentrations of coumarin-6 (0.02, 0.05 and 0.2 µg/mL). After incubation, the solution was discarded. These cells were washed with cold PBS solution, and then solubilized in 200 µL PBS solution containing 1% (v/v) TritonX-100. The fluorescence intensity was analyzed by a fluorescence microplate (OLYMPUS IX73P2F, TOKYO163-0914, Japan) at wavelengths of 470 nm (excitation) and 508 nm (emission). The cells without any treatment were used as the blank control.

2.9. Cellular proliferation inhibition assay of GA-DA-CH-Lips

The cellular proliferation inhibition assay of GA-DA-CH-Lips was evaluated by MTT. HepG2 cells were seeded in 96-well plates (5000 cells/well) with 10% FBS containing medium (100 µL/well) for 24 h at 37 °C. The medium was removed, and each well was replaced with 100 µL medium containing B-Lips or GA-DA-CH-Lips at various concentrations of GA-DA-CH (0.5, 1, 2.5, and 5 µg/mL). After treatment for 24 h, the residual medium was removed and 20 µL of MTT solution (5 mg/mL) was added into each well, and the cells were incubated for another 4 h at 37 °C. The MTT solution was discarded, and 150 µL of dimethyl sulfoxide was added into each well. The absorbance of cell viability was determined by a microplate reader (BioTek Instruments Inc., VT). Cell viability rate (%) was calculated by using the absorbance of treated cells at each concentration compared to untreated cells as a control group.

2.10. Statistical analysis

The results were expressed as the mean \pm standard deviation of three replications. All statistical analyses were performed using GraphPad Prism 6 software. Statistical comparisons between two groups were performed using the student's *t*-test, and multiple comparisons were performed using one-way analysis of variance (ANOVA) and Tukey's multiple comparison tests. Data were considered statistically significant at $P < 0.05$.

3. Results and discussion

3.1. Synthesis of GA-DA-CH

GA-DA-CH was successfully synthesized by the acylation reaction in organic media described in Scheme 1. The synthesis steps were monitored by TLC to ensure completion of the reaction. The molecular weight detected was 653.5610 $[M + H]^+$ by ESI-MS (positive-ion mode), which suggested that the product obtained was GA-DA (calculated molecular weight of 652.5543). Moreover, the molecular weight detected was 1119.7506 $[M - H]^-$ by APCI-MS (negative-ion mode), which indicated that GA-DA-CH (calculated molecular weight of 1120.9146) was synthesized successfully. In addition, GA-DA and GA-DA-CH were further characterized by 1H NMR analysis. The characteristic signal of protons in $CDCl_3$ appeared approximately at δ_H 7.26 ppm. Based on the spectra, we could identify a single peak at δ_H 5.64 ppm was attributed to the protons in the olefinic bond ($-[C = O]-CH = C-$) of GA. The peak at δ_H 1.26–2.69 ppm was attributed to the protons of alkyl unit ($-CH_2-CH_2-$) in the chain of 1,12-diaminododecane. All these marker signals were found in the 1H NMR spectrum of GA-DA. Moreover, the peak at δ_H 5.74 ppm, which was apparent only in the spectrum of GA-DA, resulted from the $-NH_2$ group of 1,12-diaminododecane, indicating a successful amidation reaction between GA and 1,12-diaminododecane. Similarly, in the synthesis of GA-DA-CH, the peak at δ_H 7.17 ppm was attributed to the other proton of the $-NH_2$ group. This finding indicated a successful amidation reaction between GA-DA and cholesteryl hemisuccinate.

GA-DA-CH was further characterized by ^{13}C NMR analysis. We found that the amidation at the primary amine group was shifted to show a higher magnetic field of the peak corresponding to O-acylated carbon atom and its neighboring carbon atom. The carboxyl group ($-COOH$) on GA reacted with the amino group ($-NH_2$) of 1,12-dodecanediamine ($NH_2-(CH_2)_{12}-NH_2$) to form the amide bond ($-CO-NH$). The chemical shift value at one O-acylated carbon atom was shifted to a higher magnetic field, about 7.12 ppm (from δ_C 182.7 ppm to δ_C 175.58 ppm). Meanwhile, neighboring carbon atoms were also shifted to a higher magnetic field, about 2.5 ppm (from δ_C 42.0 ppm to δ_C 39.52 ppm) and a 5.0 ppm (from δ_C 42.5 ppm to δ_C 37.5 ppm), indicating that acylation occurred between GA and 1,12-diaminododecane. The ^{13}C NMR spectrum of GA-DA-CH showed that the peak of 12.8 ppm disappeared. Moreover, the chemical shift value at the other O-acylated carbon atom was shifted to a higher magnetic field, about 1.59 ppm (from 174.70 ppm to 173.11 ppm), indicating that amidation was successful. The product was

proved to be GA-DA-CH, which was synthesized from GA, 1,12-diaminododecane and cholesteryl hemisuccinate in organic phase.

3.2. FTIR analysis of GA-DA-CH

The synthesized compound of GA-DA-CH was subjected to FTIR analysis. As shown in Fig. 1, the main characteristic peaks of GA were seen at 3440.89 cm^{-1} (O–H bond stretching) and 1654.32 cm^{-1} (C = C bond stretching). Meanwhile, the absorption peaks of methylene during asymmetrical stretching of GA-DA and GA-DA-CH were observed within the range of 2853.43 cm^{-1} to 2929.65 cm^{-1} . The methylene stretching vibration reflected the internal structure of the GA-DA-CH, and indicated that 1,12-diaminododecane and cholesteryl hemisuccinate stabilized the GA. In addition, peaks at $1735.72\text{ cm}^{-1}/1704.57\text{ cm}^{-1}$ represented the stretching vibrations of C = O bond. The weakening of the C = O bond peak intensity further indicated the formation of hydrogen bonds between GA-DA and carbonyl group of cholesteryl hemisuccinate. Moreover, after acylation occurred in GA, 1,12-diaminododecane and cholesteryl hemisuccinate, the N–H wavenumber of GA-DA-CH shifted from 3404.43 cm^{-1} to 3338.12 cm^{-1} . Thus, all these results implied that GA had been combined with 1,12-diaminododecane and cholesteryl hemisuccinate to successfully form GA-DA-CH.

3.3. HPLC method for the analysis of GA-DA-CH

A simple method, HPLC, was specific to determine GA-DA-CH. The typical HPLC chromatogram of GA-DA-CH is shown in Fig. 2. GA-DA-CH, GA-DA, and cholesteryl hemisuccinate were eluted at 11.5 min, 3.1 min, and 6.5 min, respectively, with satisfactory peak resolution, indicating that the method was selective and effective. The run time for the developed chromatographic method was flexible and reasonable (within 13 min). Liquid chromatography parameters which control the separation of analytes including GA-DA-CH and its substrates (GA-DA and cholesteryl hemisuccinate) were determined. The absorption wavelength and mobile phase were adjusted. For the quantitative determination of GA by HPLC, the absorption wavelength was 250 nm. The retention time of GA was 5–6 min under the mobile phase of methanol-1% acetic acid (89:11, v:v). However, GA-DA-CH was eluted at 70 min under the same conditions, indicating that the detection parameters of GA were not suitable for GA derivatives. It is possible that the conjugated system of C = C bonds in GA-DA-CH is very weak, which results in absorption at the end ultraviolet wavelength. When the absorption wavelength was shifted to 210 nm and the mobile phase was changed to methanol, the retention times of GA-DA-CH, GA-DA, and cholesteryl hemisuccinate were difference, resulting in a relative short time, and therefore, the established method can be used for GA-DA-CH quantification.

3.4. Physicochemical characterization of GA-DA-CH-Lips

3.4.1. Morphological measurement

GA-DA-CH-Lips were characterized by TEM. The morphology image and particle size of GA-DA-CH-Lips are shown in Fig. 3. GA-DA-CH-Lips droplets stained with phospho-

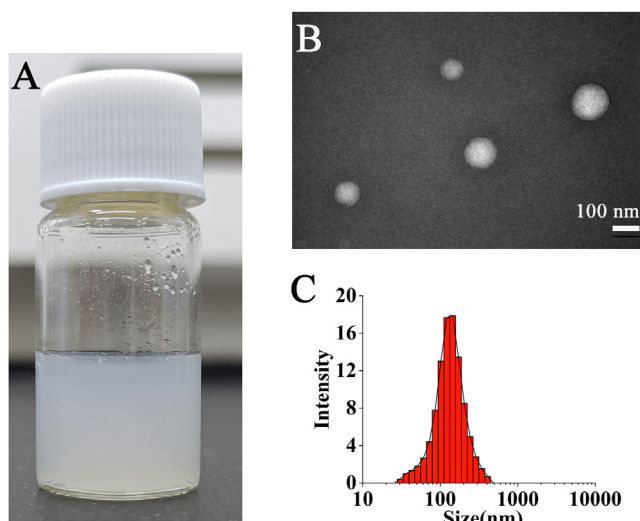


Fig. 3 Morphology and particle size of GA-DA-CH-Lips.

lower than blank controls. The positively charged amino group of GA-DA-CH can interact with the negatively charged lipid membranes phosphate groups. Thus, the decrease of zeta potential values could be due to the presence of GA-DA-CH containing diaminododecane, as we found that GA-DA-CH-Lips density was negatively correlated with zeta potential. Indeed, the vesicles of GA-DA-CH-Lips presented lower zeta potential values than blank liposomes, indicating that electrostatic interactions between GA-DA-CH and liposomal surfaces may occur.

3.4.3. Encapsulation efficiency and drug loading analysis

We note that the encapsulation efficiency of all GA-DA-CH-Lips were above 90% (Table 1). The encapsulation efficiency of three batches of GA-DA-CH-Lips was 90.85 ± 0.85 , 90.45 ± 1.56 , and 93.48 ± 0.92 . These liposomes showed a higher encapsulation rate. Moreover, the drug loading of GA-DA-CH-Lips was above 6.40%, indicating that GA-DA-CH was efficiently encapsulated in liposomes. This maybe because the negatively charged lipids tend to increase the inter-bilayer distance due to the increasing electrostatic repulsion among phosphate head groups, thus accommodating more ligands in the space generated. As a result, GA-DA-CH incorporates the double-layer structure of phospholipid during the preparation process, thus reducing the occurrence of leakage. This finding is consistent with the results of previously published reports (Chen et al., 2021).

3.5. Stability of GA-DA-CH-Lips

Environmental temperature and storage time are essential factors affecting the stability parameters of the conventional lipo-

somes. The stability of GA-DA-CH-Lips showed changes in particle size, encapsulation efficiency, and drug loading during storage at 4 °C and 26 °C for 28 days. Fig. 4 shows the variation of stability of GA-DA-CH-Lips under different storage times and environmental temperature. All freshly prepared liposomal samples remained good physicochemical properties. The changes in particle size of GA-DA-CH-Lips during 4 °C and 26 °C storage are shown in Fig. 4A. There is no significant difference in particle size during the first 14 days of storage for both samples (P greater than 0.05). During extended storage, the particle size slightly increased until the end of storage. The particle size ranged from 128.08 nm to 158.98 nm (4 °C) and 128.05 nm to 140.93 nm (26 °C), which was still within acceptable categories for liposomes. We speculated that the thermal movement of molecules still occurred in the liposomal system, which caused the particles to collide with one another or aggregate into larger particles over time. This finding was consistent with the results reported previously (Wang et al., 2022; Chotphruethipong et al., 2020). In addition, the instability of conventional liposomes due to events including oxidation or hydrolysis of lipid components in a hydrophilic system could stimulate the aggregation or fusion of liposomes (Wang et al., 2022; Khan et al., 2018).

The variation in encapsulation efficiency and drug loading of GA-DA-CH-Lips during the storage at 4 °C and 26 °C for 28 days is depicted in Fig. 4B–C. The encapsulation efficiency of GA-DA-CH-Lips in freshly prepared liposomes was above 90%. Overall, a significant decrease in encapsulation efficiency and drug loading of GA-DA-CH-Lips stored at room temperature (26 °C) was observed as the time increased ($P < 0.01$). For samples of GA-DA-CH-Lips stored at 26 °C for 28 days, the encapsulation efficiency and drug loading significantly decreased to 44.58% and 3.30%, respectively, which means its leakage rate was as high as 48.30%. This change is perhaps due to the increased temperature, which created an unstable system that accelerated Ostwald ripening. Environmental temperatures could increase the thermal energy of the liposomal droplets and gradual destabilization of liposome-water interface films. Subsequently, the frequency of droplet collisions increases (Li et al., 2016). This resulted in accelerated release rate and diffusion coefficient of core materials such as GA-DA-CH. Therefore, this led to decreased encapsulation efficiency and drug loading of GA-DA-CH-Lips, which may be caused by the leakage of liposomes. The sensitivity of encapsulation efficiency, drug loading, and leaking rate to temperature imply that GA-DA-CH-Lips should be preserved at lower temperature.

3.6. In vitro cellular uptake of GA-DA-CH-Lips

The qualitative cellular uptake of HepG2 cells after incubation with Cou6-GA-DA-CH-Lips by fluorescence microscopy are shown in Fig. 5. The morphology and distribution of HepG2 cells were observed in the bright field (Fig. 5 (A1, B1, C1

Table 1 Characterizations of GA-DA-CH-Lips by qualitative analysis.

Bath number	Particles size (nm)	PDI	Zeta potential (mV)	Encapsulation efficiency (%)	Drug loading (%)
20220725	122.87 ± 5.39	0.22 ± 0.04	-32.50 ± 1.81	90.85 ± 0.85	6.40 ± 0.06
20220805	133.30 ± 3.39	0.18 ± 0.05	-28.95 ± 1.63	90.45 ± 1.56	6.73 ± 0.11
20220815	124.97 ± 0.75	0.24 ± 0.04	-26.53 ± 1.12	93.48 ± 0.92	6.51 ± 0.06

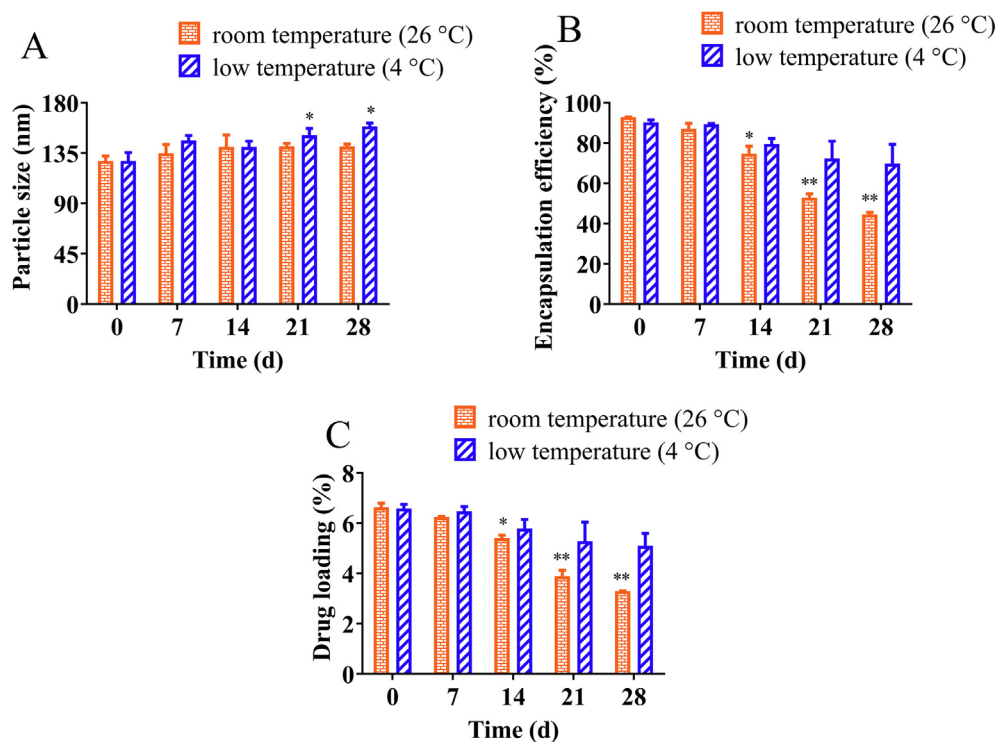


Fig. 4 The stability of GA-DA-CH-Lips under conventional storage condition including room temperature (26 °C) and low temperature (4 °C). (A) particle size, (B) encapsulation efficiency, (C) drug loading. *, compared with 0 days, $P < 0.05$; **, compared with 0 days, $P < 0.01$.

and D1)). After HepG2 cells were stained by DAPI, hepatocellular nuclei were shown with blue fluorescence (Fig. 5 (A2, B2, C2 and D2)). HepG2 cells were observed using green fluorescence under a fluorescence microscope while the fluorescent dye of coumarin-6 was absorbed in cells. We found that the green fluorescence intensity of Cou6-Lips was weak when the concentration of coumarin-6 was 0.1 $\mu\text{g}/\text{mL}$ (Fig. 5A3). The green fluorescence intensity increased significantly when GA-DA-CH modified Cou6-Lips (Fig. 5B3) at the same concentration. Meanwhile, a similar result was obtained when the concentration of coumarin-6 was 0.2 $\mu\text{g}/\text{mL}$. These results showed that the uptake efficiency of Cou6-GA-DA-CH-Lips by HepG2 cells was significantly higher than that of conventional liposomes (Cou6-Lips), suggesting that this selective targeting effect was attributed to the ligand of GA-DA-CH, which is specifically recognized by GA receptors on the surface of HepG2 cells. We speculated that GA-DA-CH could enhance cellular localization and interaction of liposomes by the endocytosis mechanism of specific GA receptors on HepG2 cells. Thus GA-DA-CH functionalized liposomes could improve the cellular uptake rate mediated by GA receptors. Endocytosis was regarded as a route of uptake for GA ligand materials in different cell lines, which was confirmed in these reports previous (Sun et al. 2017, Zhu et al. 2020).

Furthermore, we determined the intracellular GA-DA-CH efficiency to determine whether or not the uptake of GA-DA-CH-Lips could be promoted in HepG2 cells. The cellular uptake of Cou6-GA-DA-CH-Lips in HepG2 cells was analyzed using a fluorescence microplate reader. As shown in Fig. 6, the mean fluorescence intensity of Cou6-GA-DA-CH-Lips was significantly higher than that of Cou6-Lips

($P < 0.05$) in HepG2 cells. Moreover, the fluorescence intensity values of Cou6-GA-DA-CH-Lips were 14940 ± 599 , 33448 ± 1513 , and 73521 ± 3732 . Compared with those of Cou6-Lips, the cellular uptake effects of Cou6-GA-DA-CH-Lips on HepG2 cells were increased by 1.73 times, 1.41 times, and 1.44 times respectively. The results obtained from the fluorescence microplate experiment were consistent with the fluorescence microscopy analysis. This further confirmed that the synthesized ligand of GA-DA-CH could enhance cell binding and internalization of liposomes into the over-expressed GA receptors on hepatocellular carcinoma, which result in the superior targeting effect of Cou6-GA-DA-CH-Lips on HepG2 cells.

Based on these results from both qualitative and quantitative analysis of cellular uptake, we concluded that liposomes modified with GA-DA-CH ligand could effectively facilitate *in vitro* cellular uptake of HepG2 cells mediated by GA receptors, which may be attributed to the GA receptor-mediated endocytosis. Therefore, the selective accumulation of GA-DA-CH ligand functional liposomes provides specific targeting for hepatocellular carcinoma, which could promote drug uptake by HepG2 cells and improve therapeutics efficiency.

3.7. Cellular proliferation inhibition assay of GA-DA-CH-Lips

The *in vitro* cellular proliferation inhibition of GA-DA-CH-Lips against HepG2 cells was evaluated by the MTT assay. As shown in Fig. 7, we noticed that the cell viability percentage of B-Lips was more than 95%. There was no significant proliferation inhibition difference observed for B-Lips against

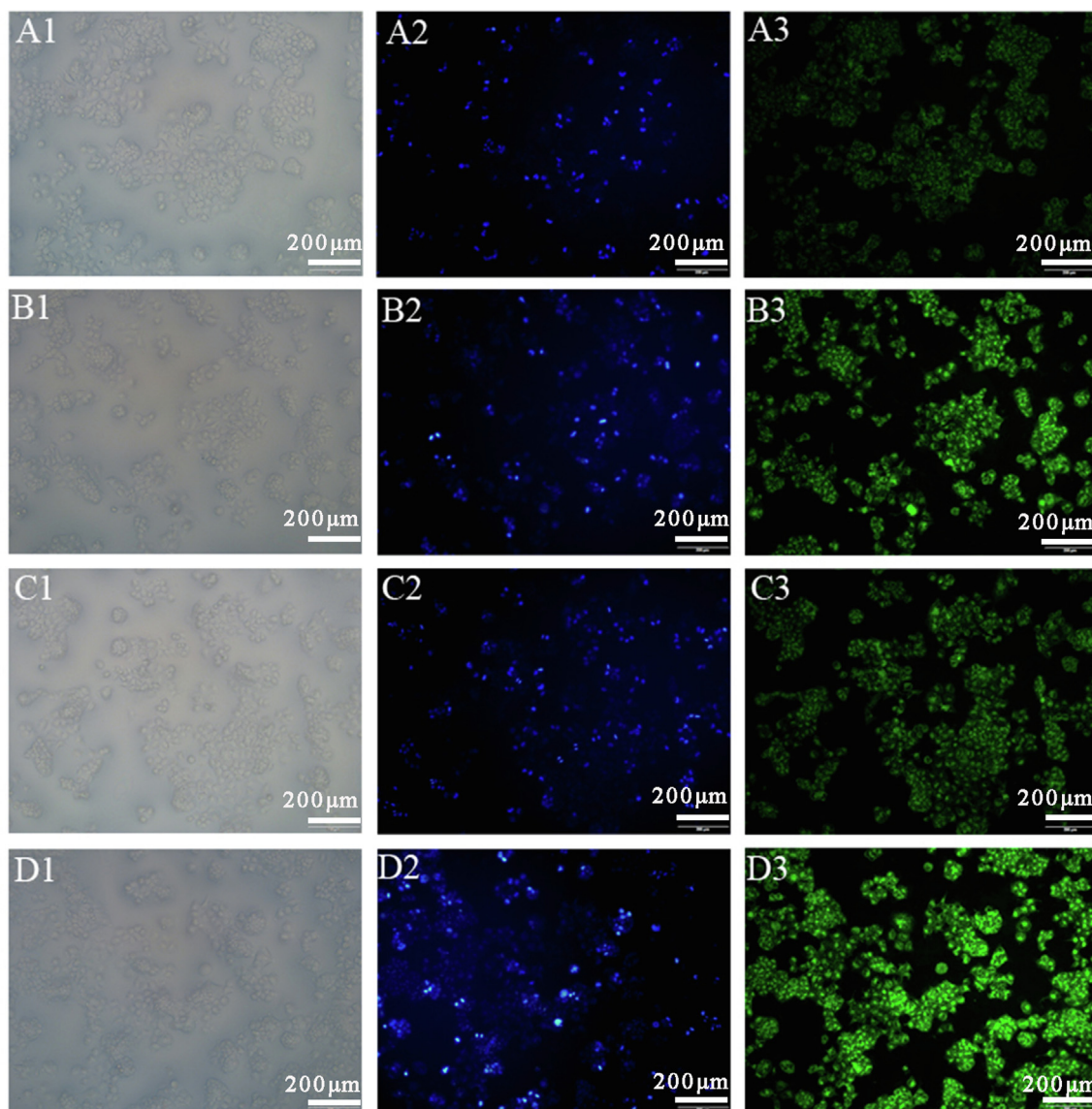


Fig. 5 Cellular uptake of HepG2 cells after incubation with Cou6-GA-DA-CH-Lips and Cou6-Lips. Bright field image in Column 1 shows the cells' distribution, and blue fluorescence in column 2 shows DAPI nuclear staining of HepG2 cells. Green fluorescence in column 3 indicates cellular uptake efficiency of Cou6. A-D groups are different experimental conditions. (A) Cou6-Lips (0.1 µg/mL), (B) Cou6-GA-DA-CH-Lips (0.1 µg/mL), (C) Cou6-Lips (0.2 µg/mL), (D) Cou6-GA-DA-CH-Lips (0.2 µg/mL).

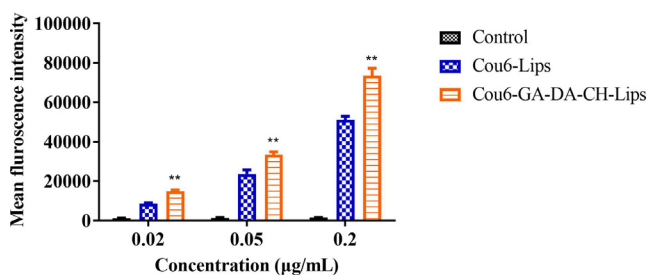


Fig. 6 Mean fluorescence intensity of treated cells incubated with Cou6-GA-DA-CH-Lips and Cou6-Lips using a fluorescence microplate. **, compared with Cou6-Lips and control, $P < 0.05$.

HepG2 cells with increasing concentration (P greater than 0.05), indicating that B-Lips were biocompatible and suitable as a potential drug delivery system. It was observed that the hepatocellular carcinoma targeting property of GA-DA-CH-Lips inhibited the cells proliferation in a dose dependent feature within the concentration range of 0.5 µg/mL to 5 µg/mL compared to B-Lips. Cell viability percentage for different concentration of GA-DA-CH-Lips was 100.10 ± 17.12 (0.5 µg/mL), 103.87 ± 16.48 (1 µg/mL), 86.36 ± 9.14 (2.5 µg/mL), and 76.99 ± 9.27 (5 µg/mL), indicating the decrease in cellular viability by increasing the concentration of GA-DA-CH. When comparing the same concentration group in both exposures (2.5 µg/mL and 5 µg/mL), GA-DA-CH-Lips exhibited higher desirable anti-proliferation efficacy in HepG2 cells as compared with B-Lips, which was a signifi-

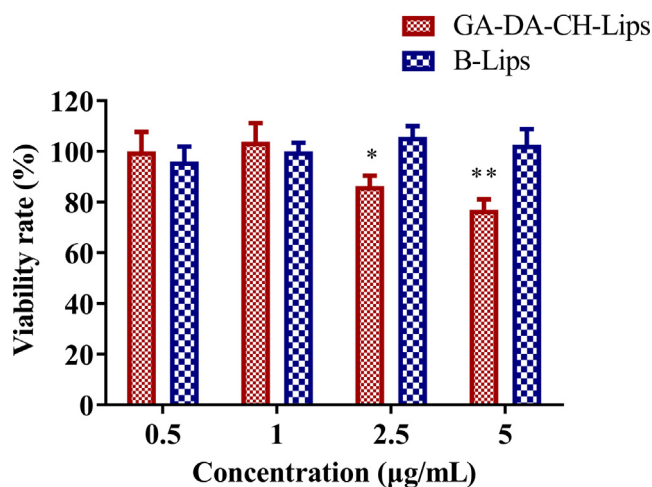


Fig. 7 Proliferation inhibition of GA-DA-CH-Lips and B-Lips against HepG2 cells evaluated by the MTT assay. *, $P < 0.05$, compared with the same concentration group of B-Lips. **, $P < 0.01$, compared with the same concentration group of B-Lips.

cantly statistical difference ($P < 0.05$). GA-DA-CH modification increased the cellular proliferation inhibition in the liposomes, which may be associated with the interaction between GA-DA-CH and GA receptors on the hepatocellular membrane. This is probably the reason that GA-DA-CH ligand functionalized liposome-mediated cellular endocytosis could enhance the hepatocellular uptake of chemotherapy drugs. GA-DA-CH-Lips can effectively improve the uptake effect of HepG2 cells via GA-DA-CH loaded liposomes through the endocytosis mechanism mediated by GA receptors, thus resulting in GA-DA-CH-Lips having a significant anti-proliferation effect on hepatocellular carcinoma.

4. Conclusion

In this study, we successfully designed a novel GA derivate compound as functional material for liposomal modification. GA-DA-CH was synthesized from GA, 1,12-diaminododecane, and cholesterol succinate monoester by two-step amidation under catalytic conditions. The physicochemical structures of GA-DA-CH were confirmed by MS, NMR, and FTIR. In addition, we established a simple method of HPLC analysis to determine the content of GA-DA-CH within 13 min. Functional liposomes of GA-DA-CH-Lips were developed by thin-film method, consisting of egg phosphatidylcholine, cholesterol and GA-DA-CH, and the GA-DA-CH ligand was integrated into the liposomal capsule to enhance hepatocellular carcinoma targeting. These liposomal characterizations of GA-DA-CH-Lips were desirable with particle sizes ranging from 122.87 nm to 133.30 nm, PDI close to 0.20, zeta potential in the range of -32.50 mV to -26.53 mV, and encapsulation efficiency more than 90% and drug loading $\text{no} < 6.40\%$. Moreover, the stability of GA-DA-CH-Lips was evaluated, and the results suggested that these liposomes should be stored at low temperatures to retain stable properties and prolong their shelf life. Furthermore, we investigated target efficiency to confirm that the uptake of GA-DA-CH-Lips could be promoted in HepG2 cell. The cellular uptake results obtained from qualitative and qualitative analysis indicated that GA-DA-CH accelerated uptake of coumarin-6, a fluorescent drug substitute in HepG2 cells, demonstrating that the synthesized ligand of GA-DA-CH integrated into liposomes possesses a

specific targeting ability for hepatocellular carcinoma. In the cellular inhibition assay of GA-DA-CH-Lips, we concluded that GA-DA-CH-Lips can effectively improve the cellular uptake effect of the HepG2 cells-mediated endocytosis mechanism by GA receptors, so GA-DA-CH-Lips exhibited a stronger anti-proliferation efficacy as compared with blank liposomes. These results support our hypothesis that functional liposomes containing GA-DA-CH are a promising potential drug target delivery system to improve the therapeutic efficiency of hepatic diseases treatments.

Declaration of Competing Interest

The authors declare that they have no known competing financial interests or personal relationships that could have appeared to influence the work reported in this paper.

Acknowledgments

This research was funded by the Science and Technology Project of Jiangmen City, China (grant number 2021030102600004808), the Project of Doctoral Research Initiation in Wuyi University, China (grant number 5041700109), and the Project of Innovative and Entrepreneurship in Wuyi University, China (grant number 2022CX30, 2022CX27, 2019CX13), Hongkong and Macao associated Research and development Fund of Wuyi University, China (grant number 2021W GALH10).

Appendix A. Supplementary material

Supplementary data to this article can be found online at <https://doi.org/10.1016/j.arabjc.2023.105131>.

References

- Aoki, T., Kubota, K., Hasegawa, K., Kubo, S., Izumi, N., Kokudo, N., Sakamoto, M., Shiina, S., Takayama, T., Nakashima, O., Matsuyama, Y., Murakami, T., Kudo, M., 2020. Significance of the surgical hepatic resection margin in patients with a single hepatocellular carcinoma. *Brit. J. Surg.* 107, 113–120. <https://doi.org/10.1002/bjs.11329>.
- Beltrán-Gracia, E., López-Camacho, A., Higuera-Ciajara, I., Velázquez-Fernández, J.B., Vallejo-Cardona, A.A., 2019. Nanomedicine review: clinical developments in liposomal applications. *Cancer Nanotechnol.* 10, 11–50. <https://doi.org/10.1186/s12645-019-0055-y>.
- Cai, H.K., Chen, X., Zhang, J.B., Wang, J.J., 2018. 18β-glycyrrhetic acid inhibits migration and invasion of human gastric cancer cells via the ROS/PKC-α/ERK pathway. *J. Nat. Med.* 72, 252–259. <https://doi.org/10.1007/s11418-017-1145-y>.
- Cai, Y.E., Xu, Y.Q., Chan, H.F., Fang, X.B., He, C.W., Chen, M.W., 2016. Glycyrrhetic acid mediated drug delivery carriers for hepatocellular carcinoma therapy. *Mol. Pharmaceutics* 13, 699–709. <https://doi.org/10.1021/acs.molpharmaceut.5b00677>.
- Chen, J., Chen, Y.C., Cheng, Y., Gao, Y.H., 2017. Glycyrrhetic acid liposomes containing mannose-diester lauric diacid-cholesterol conjugate synthesized by lipase-catalytic acylation for liver-specific delivery. *Molecules* 22, 1598–1617. <https://doi.org/10.3390/molecules22101598>.
- Chen, J., Chen, Y.C., Cheng, Y., Gao, Y.H., Zheng, P.J., Li, C.N., Tong, Y.D., Li, Z., Luo, W.H., Chen, Z., 2017. Modifying glycyrrhetic acid liposomes with liver-targeting ligand of galactosylated derivative preparation and evaluations. *Oncotarget* 8, 1002046–1102066. <https://doi.org/10.18632/oncotarget.22143>.

- Chen, J., Zhang, Z.Q., Song, J., Liu, Q.M., Wang, C., Huang, Z., Chu, L., Liang, H.F., Zhang, B.X., Chen, X.P., 2018. 18 β -Glycyrrhetic-acid-mediated unfolded protein response induces autophagy and apoptosis in hepatocellular carcinoma. *Sci. Rep.* 8, 9365–9377. <https://doi.org/10.1038/s41598-018-27142-5>.
- Chen, J., Lin, Y., Wu, M., Li, C.N., Zhang, Y.M., Chen, D.P., Cheng, Y., 2021. Drug-free liposomes containing mannoseylated ligand for liver-targeting: Synthetic optimization, liposomal preparation, and bioactivity evaluation. *J. Biomed. Nanotechnol.* 17, 2455–2465. <https://doi.org/10.1166/jbn.2021.3204>.
- Chen, J., Lin, Y., Wu, M., Li, C.N., Cen, K.J., Liu, F.J., Liao, Y.Z., Zhou, X.Q., Xu, J.C., Cheng, Y., 2022. Glycyrrhetic acid liposomes mediated by mannoseylated ligand: Preparation, physicochemical characterization, environmental stability and bioactivity evaluation. *Colloid Surf. B* 218, 112781–112790. <https://doi.org/10.1016/j.colsurfb.2022.112781>.
- Chotphruethipong, L., Battino, M.A., Benjakul, S., 2020. Effect of stabilizing agents on characteristics, antioxidant activities and stability of liposome loaded with hydrolyzed collagen from defatted Asian sea bass skin. *Food Chem.* 328, 127127–127161. <https://doi.org/10.1016/j.foodchem.2020.127127>.
- Cucchetti, A., Zhong, J.H., Berhane, S., Toyoda, H., Shi, K.Q., Tada, T., Chong, C.C.N., Xiang, B.D., Li, L.Q., Lai, P.B.S., Ercolani, G., Mazzaferro, V., Kudo, M., Cescon, M., Pinna, A.D., Kumada, T., Johnson, P.J., 2020. The chances of hepatic resection curing hepatocellular carcinoma. *J. Hepatol.* 72, 711–717. <https://doi.org/10.1016/j.jhep.2019.11.016>.
- Domingues, M.M., Santiago, P.S., Castanho, M.A.R.B., Santos, N.C., 2008. What can light scattering spectroscopy do for membrane-active peptide studies? *J. Pept. Sci.* 14, 394–400. <https://doi.org/10.1002/psc.1007>.
- Farooq, M.A., Huang, X.Y., Jabeen, A., Ahsan, A., Seidu, T.A., Kutoka, P.T., Wang, B., 2021. Enhanced cellular uptake and cytotoxicity of vorinostat through encapsulation in TPGS-modified liposomes. *Colloid Surf. B* 199, 111523–112132. <https://doi.org/10.1016/j.colsurfb.2020.111523>.
- Guimaraes, D., Cavaco-Paulo, A., Nogueira, E., 2021. Design of liposomes as drug delivery system for therapeutic applications. *Int. J. Pharmaceut.* 601, 120571–120585. <https://doi.org/10.1016/j.ijpharm.2021.120571>.
- Guo, Y.S., Ren, Y.Q., Chen, L., Sun, T., Zhang, W.H., Sun, B., Zhu, L.C., Xiong, F., Zheng, C.S., 2022. Transarterial chemoembolization combined with camrelizumab for recurrent hepatocellular carcinoma. *BMC Cancer* 22, 270–277. <https://doi.org/10.1186/s12885-022-09325-6>.
- Hou, Z.Q., Liu, J., Jin, Z.X., Qiu, G.T., Xie, Q.Y., Mi, S.Z., Huang, J.W., 2022. Use of chemotherapy to treat hepatocellular carcinoma. *Biosci. Trends* 16, 31–45. <https://doi.org/10.5582/bst.2022.01044>.
- Huang, S.X., Ren, D., Wu, X.R., Li, M., Yu, X.S., Nie, X.L., Wang, Y., Wang, Y., 2020. Glycyrrhetic acid and TAT peptide modified dual-functional liposomes for treatment of hepatocellular cancer. *Curr. Top. Med. Chem.* 20, 2493–2505. <http://doi.org/10.2174/1568026620666200722110244>.
- Jaafar-Maalej, C., Diab, R., Andrieu, V., Elaissari, A., Fessi, H., 2010. Ethanol injection method for hydrophilic and lipophilic drug-loaded liposome preparation. *J. Liposome Res.* 20, 228–243. <http://doi.org/10.3109/08982100903347923>.
- Kakos, C.D., Ziogas, I.A., Demiri, C.D., Esagian, S.M., Economopoulos, K.P., Moris, D., Tsoulfas, G., Alexopoulos, S.P., 2022. Liver transplantation for pediatric hepatocellular carcinoma: A systematic review. *Cancers* 14, 1294–1311. <https://doi.org/10.3390/cancers14051294>.
- Kamimura, K., Terai, S., 2021. The promise of radiotherapy for hepatocellular carcinoma. *Hepatol. Res.* 51, 837–838. <https://doi.org/10.1111/hepr.13687>.
- Khan, I., Yousaf, S., Subramanian, S., Alhnan, M.A., Ahmed, W., Elhissi, A., 2018. Liposome tablets manufactured using a slurry-driven lipid-enriched powders: Development, characterization and stability evaluation. *Int. J. Pharmaceut.* 538, 250–262. <http://doi.org/10.1016/j.ijpharm.2017.12.049>.
- Kim, B., Kahn, J., Terrault, N.A., 2020. Liver transplantation as therapy for hepatocellular carcinoma. *Liver Int.* 40, 116–121. <https://doi.org/10.1111/liv.14346>.
- Lekar, A.V., Maksimenko, E.V., Borisenko, S.N., Khizrieva, S.S., Vetrova, E.V., Borisenko, N.I., Minkin, V.I., 2019. One-pot synthesis of glycyrrhetic acid from licorice root in subcritical water. *Russ. J. Phys. Chem. B* 13, 1150–1154. <http://doi.org/0.1134/s1990793119070170>.
- Li, P.H., Lu, W.C., 2016. Effects of storage conditions on the physical stability of d-limonene nanoemulsion. *Food Hydrocolloid* 53, 218–224. <https://doi.org/10.1016/j.foodhyd.2015.01.031>.
- Li, J.R., Malhotra, A., Bi, J.G., 2019. Potential of ablation therapy during hepatocellular carcinoma. *Nutr. Cancer* 71, 881–885. <https://doi.org/10.1080/01635581.2018.1531137>.
- Luo, Y.H., Wang, C., Xu, W.T., Zhang, Y., Zhang, T., Xue, H., Li, Y. N., Fu, Z.R., Wang, Y., Jin, C.H., 2021. 18 β -Glycyrrhetic acid has anti-cancer effects via inducing apoptosis and G2/M cell cycle arrest, and inhibiting migration of A549 lung cancer cells. *Oncotargets Ther.* 14, 5131–5144. <https://doi.org/10.2147/ott.s322852>.
- Lv, Y.J., Li, J.J., Chen, H.L., Bai, Y., Zhang, L.K., 2017. Glycyrrhetic acid-functionalized mesoporous silica nanoparticles as hepatocellular carcinoma-targeted drug carrier. *Int. J. Nanomed.* 12, 4361–4370. <https://doi.org/10.2147/ijn.s135626>.
- Marwah, M., Narain Srivastava, P., Mishra, S., Nagarsenker, M., 2020. Functionally engineered 'hepato-liposomes': Combating liver-stage malaria in a single prophylactic dose. *Int. J. Pharmaceut.* 587, 119710–119722. <https://doi.org/10.1016/j.ijpharm.2020.119710>.
- Mu, W.W., Chu, Q.H., Liu, Y.J., Zhang, N., 2020. A review on nano-based drug delivery system for cancer chemoimmunotherapy. *Nano-Micro Lett.* 12, 142–165. <https://doi.org/10.1007/s40820-020-00482-6>.
- Negishi, M., Irie, A., Nagata, N., Ichikawa, A., 1991. Specific binding of glycyrrhetic acid to the rat liver membrane. *Biochim. Biophys. Acta* 1066, 77–82. [https://doi.org/10.1016/0005-2736\(91\)90253-5](https://doi.org/10.1016/0005-2736(91)90253-5).
- Paganoni, R., Lechel, A., Vujic Spasic, M., 2021. Iron at the interface of hepatocellular carcinoma. *Int. J. Mol. Sci.* 22, 4097–4111. <https://doi.org/10.3390/ijms22084097>.
- Pastorino, G., Cornara, L., Soares, S., Rodrigues, F., Oliveira, M., 2018. Licorice (*Glycyrrhiza glabra*): A phytochemical and pharmacological review. *Phytother. Res.* 32, 2323–2339. <https://doi.org/10.1002/ptr.6178>.
- Seidi, K., Neubauer, H.A., Moriggl, R., Jahanban-Esfahlan, R., Javaheri, T., 2018. Tumor target amplification: Implications for nano drug delivery systems. *J. Control. Release* 275, 142–161. <https://doi.org/10.1016/j.jconrel.2018.02.020>.
- Sharma, G., Kar, S., Palit, S., Das, P.K., 2012. 18 β -glycyrrhetic acid induces apoptosis through modulation of Akt/FOXO3a/Bim pathway in human breast cancer MCF-7 cells. *J. Cell. Physiol.* 227, 1923–1931. <https://doi.org/10.1002/jcp.22920>.
- Speciale, A., Muscara, C., Molonia, M.S., Cristani, M., Cimino, F., Saija, A., 2022. Recent advances in glycyrrhetic acid-functionalized biomaterials for liver cancer-targeting therapy. *Molecules* 27, 1775–1802. <https://doi.org/10.3390/molecules27061775>.
- Stecanella, L.A., Bitencourt, A.P.R., Vaz, G.R., Quarta, E., Silva Junior, J.O.C., Rossi, A., 2021. Glycyrrhetic acid and its hydrolyzed metabolite 18 β -Glycyrrhetic acid as specific ligands for targeting nanosystems in the treatment of liver cancer. *Pharmaceutics* 13, 1792–1814. <https://doi.org/10.3390/pharmaceutics13111792>.
- Sun, Y., Jiang, M., Park, P.H., Song, K., 2020. Transcriptional suppression of androgen receptor by 18 β -glycyrrhetic acid in LNCaP human prostate cancer cells. *Arch Pharm. Res.* 43, 433–448. <https://doi.org/10.1007/s12272-020-01228-z>.
- Sun, Y.Q., Lu, J.H., Yan, D.X., Shen, L.P., Hu, H.Y., Chen, D.W., 2017. Cellular uptake mechanism and clearance kinetics of

- fluorescence-labeled glycyrrhetic acid and glycyrrhetic acid-modified liposome in hepatocellular carcinoma cells. *Environ. Toxicol. Phar.* 53, 46–56. <https://doi.org/10.1016/j.etap.2017.05.003>.
- Sung, H., Ferlay, J., Siegel, R.L., Laversanne, M., Soerjomataram, I., Jemal, A., Bray, F., 2021. Global Cancer Statistics 2020: GLOBOCAN estimates of incidence and mortality worldwide for 36 cancers in 185 countries. *CA Cancer J. Clin.* 71, 209–249. <https://doi.org/10.3322/caac.21660>.
- Tikhomirova, K.S., Lekar, A.V., Borisenko, S.N., Vetrova, E.V., Borisenko, N.I., Minkin, V.I., 2010. Synthesis of glycyrrhetic acid by hydrolysis of licorice root extract in subcritical water. *Russ. J. Phys. Chem. B* 4, 1125–1129. <https://doi.org/10.1134/s1990793110070122>.
- Wang, F., Pu, C., Liu, M., Li, R., Sun, Y., Tang, W., Sun, Q., Tian, Q., 2022. Fabrication and characterization of walnut peptides-loaded liposomes with three lyoprotectants: Environmental stabilities and antioxidant/antibacterial activities. *Food Chem.* 366, 130643–130654. <https://doi.org/10.1016/j.foodchem.2021.130643>.
- Wu, F., Xue, H.T., Li, X.C., Diao, W.B., Jiang, B., Wang, W.Y., Yu, W.J., Bai, J.K., Wang, Y., Lian, B., Feng, W.G., Sun, T.Y., Qu, M. H., Zhao, C.L., Wang, Y.B., Wu, J.L., Gao, Z.Q., 2020. Enhanced targeted delivery of adenine to hepatocellular carcinoma using glycyrrhetic acid-functionalized nanoparticles in vivo and in vitro. *Biomed. Pharmacother.* 131, 110682–110693. <https://doi.org/10.1016/j.biopha.2020.110682>.
- Yamagishi, S., Midorikawa, Y., Nakayama, H., Higaki, T., Moriguchi, M., Aramaki, O., Yamazaki, S., Tsuji, S., Takayama, T., 2019. Liver resection for recurrent hepatocellular carcinoma after radiofrequency ablation therapy. *Hepatol. Res.* 49, 432–440. <https://doi.org/10.1111/hepr.13293>.
- Yamamoto, S., Kondo, S., 2018. Oral chemotherapy for the treatment of hepatocellular carcinoma. *Expert Opin. Pharmacol.* 19, 993–1001. <https://doi.org/10.1080/14656566.2018.1479398>.
- Yan, T.S., Cheng, J.J., Liu, Z.J., Cheng, F., Wei, X.J., Huang, Y.D., He, J.M., 2018. Acid-sensitive polymeric vector targeting to hepatocarcinoma cells via glycyrrhetic acid receptor-mediated endocytosis. *Mat. Sci. Eng. C-Mater.* 87, 32–40. <https://doi.org/10.1016/j.msec.2018.02.013>.
- Ye, J., Yang, Y.F., Dong, W.J., Gao, Y., Meng, Y.Y., Wang, H.L., Li, L., Jin, J., Ji, M., Xia, X.J., Chen, X.G., Jin, Y.Q., Liu, Y.L., 2019. Drug-free mannoseylated liposomes inhibit tumor growth by promoting the polarization of tumor-associated macrophages. *Int. J. Nanomed.* 14, 3203–3220. <https://doi.org/10.2147/ijn.s207589>.
- Zhao, L., Liang, L.Y., Guo, M.M., Li, M., Yu, X.S., Wang, Y., Wang, Y., 2021. Hepatocellular carcinoma targeting and pharmacodynamics of paclitaxel nanoliposomes modified by glycyrrhetic acid and ferric tetroxide. *Curr. Top. Med. Chem.* 21, 1268–1284. <https://doi.org/10.2174/156802662166621090005>.
- Zhu, X.L., Huang, S.N., Li, L.H., Wang, S.S., Chen, J.Q., Guan, Y.B., Wang, B.Y., Jia, Y.Y., 2021. Glycyrrhetic acid-decorated and docetaxel-loaded thermosensitive liposomes for combination therapy against hepatocellular carcinoma. *J. Nanopart. Res.* 23, 158–173. <https://doi.org/10.1007/s11051-021-05273-7>.
- Zhu, J., Zhang, W., Wang, D.D., Li, S.Z., Wu, W., 2018. Preparation and characterization of norcantharidin liposomes modified with stearyl glycyrrhetinate. *Exp. Ther. Med.* 16, 1639–1646. <https://doi.org/10.3892/etm.2018.6416>.
- Zhu, K., Zhou, L.L., Zou, M.S., Ning, S.C., Liu, S.L., Zhou, Y.L., Du, K., Zhang, X.Q., Xia, X.H., 2020. 18-GA-Suc modified liposome loading cantharidin for augmenting hepatic specificity: Preparation, characterization, antitumor effects, and liver-targeting efficiency. *J. Pharm. Sci.* 109, 2038–2047. <https://doi.org/10.1016/j.xphs.2020.03.001>.